

# Design, synthesis and spectroscopic and crystallographic characterisation of novel functionalized pyrazole derivatives: biological evaluation for their cytotoxic, angiogenic and antioxidant activities

Achutha Dileep Kumar<sup>1</sup> · Srinivasan Bharath<sup>2</sup> · Rekha N. Dharmappa<sup>3</sup> · Shivalingegowda Naveen<sup>4</sup> · Neratur Krishnappagowda Lokanath<sup>5</sup> · Kariyappa Ajay Kumar<sup>1</sup>

Received: 7 February 2018 / Accepted: 18 April 2018  
© Springer Science+Business Media B.V., part of Springer Nature 2018

**Abstract** The current study presents the synthesis of functionalized pyrazoles (**18–29**) through 3 + 2 annulation reaction of ethyl 2-(arylidene)-3-oxobutanoates (**8–13**) with phenylhydrazine hydrochlorides (**14–17**) in acetic acid under reflux conditions. Structures of the synthesized new compounds were characterized by spectral and single-crystal X-ray diffraction studies. Preliminary assessment on their biological activities showed that compounds **19**, **23** and **28** have anticancer and antiangiogenic properties and compounds **20**, **24** and **26** have excellent diphenylpicrylhydrazyl (DPPH) radical scavenging activities. Detailed quantitative structure–activity relationship (QSAR) analysis provided insights into the molecular features that might have contributed towards increasing potency of inhibition. In summary, we present a study that has successfully demonstrated the synthesis of novel pyrazole analogues that display anticancer, antiangiogenic and DPPH free radical scavenging activities, making them lead molecules of choice for further development.

---

✉ Kariyappa Ajay Kumar  
ajaykumar@ycm.uni-mysore.ac.in

<sup>1</sup> Department of Chemistry, Yuvaraja's College, University of Mysore, Mysuru 570005, India

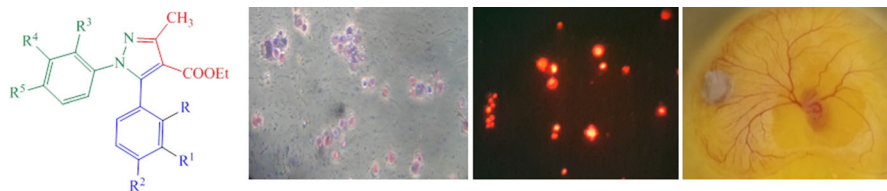
<sup>2</sup> Marie Skłodowska-Curie Actions, Rua da Quinta Grande, 6, 2780-156 Oeiras, Portugal

<sup>3</sup> Department of Biotechnology, JSS College for Arts, Commerce and Science, Ooty Road, Mysuru, India

<sup>4</sup> Department of Physics, School of Engineering and Technology, Jain University, Bangalore 562 112, India

<sup>5</sup> Department of Studies in Physics, Manasgangotri, University of Mysore, Mysuru, India

## Graphical Abstract



**Keywords** Antiangiogenic · Antioxidant · Citotoxic · Condensation · Pyrazoles

## Introduction

Cancer is a disease characterized by the progressive, persistent, abnormal and uncontrolled proliferation of cells. It is the second most dreaded cause of mortality in the world after cardiovascular disorders, and is continuing to be a major health hazard in developing as well as undeveloped countries [1]. Although there has been considerable progress to reduce cancer incidence, the number of cancer patients continues to increase. Chemotherapy is one of the most effective approaches used to treat cancer patients. However, lack of selectivity and drug resistance reduce the efficacy of cancer chemotherapy. Therefore, development of effective and safe anticancer agents with high potency and less toxicity is a major focus for researchers across the world. The most important aspects in drug design are the affinity of the small molecule for its target, the specificity of its action, drug metabolism and bioactivation. Amongst the heterocycles, pyrazoles are the scaffolds of choice in several medicinal chemistry initiatives. Derivatives of pyrazoles have been shown to possess varied properties including, but not limited to, being analgesic [2], antiarrhythmic [3], sPLA2-inhibitory [4], anti-inflammatory [5], antipyretic [6], anticancer [7], anticonvulsant [8], monoamine oxidase inhibiting [9], antidiabetic [10], and antibacterial [11]. Pyrazoles have been employed as bifunctional ligands for metal catalysis, and in various building blocks for medicinal chemistry and pharmaceutical research. Pyrazoles are synthesized by various conventional routes [12, 13]. For instance, highly regioselective synthesis of phosphonylpyrazoles by the reaction of chalcones with an  $\alpha$ -diazo- $\beta$ -ketophosphonate [14], and reaction of  $\beta$ -enaminoketoesters with phenylhydrazines via a simple and reliable approach have been successfully demonstrated [15]. The usual acid-catalyzed reaction of  $\alpha$ ,  $\beta$ -unsaturated carbonyl compounds with phenylhydrazines to produce pyrazolines is well established [16]. On the other hand, in the presence of mild bases, reaction of  $\alpha$ ,  $\beta$ -unsaturated carbonyl compounds having a benzotriazole group in the  $\alpha$  position with phenylhydrazine produces pyrazoles directly [17].

Angiogenesis is a feature of embryonal development and has prominent roles in several physiological and pathological conditions, including rheumatoid arthritis, tumor growth and metastasis, diabetic retinopathy and age-related macular

degeneration [18]. Angiogenesis-dependent diseases are controlled by using chemotherapy, immunotherapy and radiation therapy by stimulating the inhibiting factors [19]. In view of the important roles played by angiogenesis and the fact that aberrant angiogenesis can sometimes result in pathological and diseased conditions, there is additional need to synthesize small molecules regulating angiogenesis. Additionally, deleterious effects arising due to oxidative stress resulting from an imbalance between free radical generation and their quenching on human health has huge economic burden. Given the high economic costs of healthcare vis a vis treatment of conditions such as carcinogenesis, aberrant angiogenesis and free radical-mediated damage [20], in this paper, we report for the first time the direct synthesis of functionalized pyrazoles and the results of their cytotoxic, antiangiogenic and diphenylpicrylhydrazyl (DPPH) radical scavenging activities.

## Experimental

### Materials and methods

Melting points were determined by an open capillary tube method and are uncorrected.  $^1\text{H}$  Nuclear Magnetic Resonance (NMR) and  $^{13}\text{C}$  Nuclear Magnetic Resonance (NMR) spectra were recorded on Agilent 400-MHz and 100-MHz spectrometers, respectively. The chemical shifts are expressed in  $\delta$  ppm. Mass spectra were obtained on Electrospray (ESI)/Atmospheric Pressure Chemical Ionization (APCI)-Hybrid Quadrupole, Synapt G2 High Definition Mass Spectrometry (HDMS) Acquity Ultimate Performance Liquid Chromatography (UPLC) model spectrometer. Elemental analysis was obtained on a Thermo Finnigan Flash EA 1112 Elemental analyzer.

### Synthesis of benzylidene oxobutanoates, **8–13**

To a solution of aromatic aldehydes **1–6** (10 mol) and ethyl acetoacetate **7** (10 mol) in dichloromethane, a catalytic amount of piperidine (1 mL) and trifluoroacetic acid (2 mL) were added. Then the solution mixture was refluxed in a water bath for 4–5 h. The progress of the reaction was monitored by thin layer chromatography (TLVC) and after completion, the reaction mixture was cooled to room temperature and poured into ice-cold water. The products were extracted into diethyl ether (50 mL), washed successively with saturated sodium bicarbonate solution, brine solution and finally with ice-cold water. The organic layer was dried over anhydrous sodium sulphate and the solvent was evaporated in vacuo. The crude solids were recrystallized from methyl alcohol to obtain the compounds **8–13**.

### Synthesis of ethyl 1,5-diaryl-3-methyl-4,5-dihydro-1H-pyrazole-4-carboxylates, **18–29**

To a solution of ethyl 2-(4-aryl)-3-oxobutanoate, **8–13** (10 mol) and phenylhydrazine hydrochloride, **14–17** (10 mol) in acetic acid (40%) was refluxed for 5–6 h.

The progress of the reaction was monitored by thin layer chromatography (TLC). After the completion, the mixture was cooled and poured into crushed ice. The separated solids were filtered and washed successively with 5% NaHCO<sub>3</sub> and water. The crude solids were recrystallized from ethyl alcohol to get target molecules **18–29** in moderate to good yields.

### X-ray crystallography

Single crystals of suitable dimensions were chosen carefully for X-ray diffraction studies. The X-ray intensity data were collected at a temperature of 293(2) K on a Bruker Proteum2 Charge Couple Device (CCD) diffractometer equipped with an X-ray generator operating at 45 kV and 10 mA, using CuK<sub>α</sub> radiation of wavelength 1.54178 Å. Data were collected for 24 frames per set with different settings of  $\varphi$  (0° and 90°), keeping the scan width of 0.5°, exposure time of 2 s, the sample-to-detector distance of 45.10 mm and  $2\theta$  value at 46.6°. The crystal data and details concerning data collection and structure refinement are given in Table 1. Parameters in Crystallography Information File (CIF) format are available as an electronic supplementary publication from Cambridge Crystallographic Data Centre (CCDC).

### Cell culture and in vitro compounds treatment

Michigan Cancer Foundation-7 (MCF-7) breast cancer cell lines were procured from the National Centre for Cell Sciences (NCCS), Pune, India. The cells were routinely maintained in Dulbecco's Modified Eagle Medium (Sigma, St. Louis, MO, USA) supplemented with 10% heat-inactivated fetal calf serum (HiMedia, Mumbai, India). Ehrlich ascites tumour (EAT) cells were collected from JSS College of Pharmacy, Mysore.

### Trypan blue dye exclusion assay

The effects of compounds **18–29** on cell viability of MCF-7 breast cancer cell lines were determined by trypan blue dye exclusion assay. MCF-7 breast cancer cells treated with or without compounds were harvested and resuspended in 0.4% trypan blue and the viable cells were counted using haemocytometer. IC<sub>50</sub> values were estimated after 48 h of treatment.

### 3-(4,5-Dimethylthiazol-2-yl)-2,5-diphenyltetrazolium bromide (MTT) assay

The effect of compounds (**18–29**) on cell proliferation of MCF-7 breast cancer cells was determined by MTT assay according to reported procedure. Cells treated with or without compounds were incubated for 48 h. MTT reagent (5 mg/mL) was added and the color change due to proliferating cells was estimated.

**Table 1** Crystal data and structure refinement details

Compound	<b>19</b>	<b>25</b>
CCDC number	1,530,834	1,530,833
Empirical formula	C <sub>19</sub> H <sub>17</sub> FN <sub>2</sub> O <sub>2</sub>	C <sub>19</sub> H <sub>17</sub> BrN <sub>2</sub> O <sub>2</sub>
Formula weight	324.35	385.26
Temperature	296(2) K	296(2) K
Wavelength	1.54178 Å	1.54178 Å
Reflections for cell determination	2003	1700
$\theta$ range for above	5.45°–64.61°	5.45°–62.37°
Crystal system	Triclinic	Monoclinic
Space group	P $\bar{1}$	P 21/c
Cell dimensions	$a = 8.6121(5)$ Å $b = 9.8732(6)$ Å $c = 10.3398(6)$ Å $\alpha = 75.274(4)^\circ$ $\beta = 73.343(4)^\circ$ $\gamma = 76.295(4)^\circ$	$a = 10.597(2)$ Å $b = 19.861(4)$ Å $c = 8.907(2)$ Å $\alpha = 90.00^\circ$ $\beta = 109.263(15)^\circ$ $\gamma = 90.00^\circ$
Volume	801.75(8) Å <sup>3</sup>	1769.75(7) Å <sup>3</sup>
Z	2	4
Density (calculated)	1.344 Mg m <sup>-3</sup>	1.446 Mg m <sup>-3</sup>
Absorption coefficient	0.791 mm <sup>-1</sup>	3.271 mm <sup>-1</sup>
$F_{000}$	340	784
Crystal size	0.27 × 0.25 × 0.22 mm	0.29 × 0.26 × 0.22 mm
$\theta$ range for data collection	5.45°–64.61°	4.45°–62.37°
Index ranges	–10 ≤ $h$ ≤ 9 –11 ≤ $k$ ≤ 11 –12 ≤ $l$ ≤ 11	–12 ≤ $h$ ≤ 12 –22 ≤ $k$ ≤ 21 –9 ≤ $l$ ≤ 10
Reflections collected	6890	9119
Independent reflections	2630 [Rint = 0.0551]	2736 [Rint = 0.1150]
Absorption correction	Multi-scan	Multi-scan
Refinement method	Full matrix least-squares on $F^2$	Full matrix least-squares on $F^2$
Data/restraints/parameters	2630/0/219	2736/0/219
Goodness-of-fit on $F^2$	1.055	0.962
Final [ $I > 2\sigma(I)$ ]	$R1 = 0.0595$ , $wR2 = 0.1685$	$R1 = 0.0735$ , $wR2 = 0.1729$
R indices (all data)	$R1 = 0.0763$ , $wR2 = 0.1938$	$R1 = 0.1395$ , $wR2 = 0.2181$
Largest diff. peak and hole	0.325 and –0.270 e Å <sup>-3</sup>	0.537 and –0.895 e Å <sup>-3</sup>

## Chorioallantoic membrane assay

The designed series of pyrazoles (**18–29**) were screened for their antiangiogenic activity by the chorioallantoic membrane (CAM) assay according to the reported procedure. Briefly, fertilized hen eggs were surface sterilized using 70% alcohol. The eggs were incubated in a fan-assisted humidified incubator at 37 °C. On the 4th

day, the eggs were cracked into thin films of the hammock within a laminar flow cabinet and were further incubated. On the 5th day, when blood vessels were seen proliferating from the centre of the eggs within the hammock, filter paper discs loaded with 100 µg of synthesized pyrazoles were placed over the proliferating blood vessels and the eggs were returned to the incubator. Results for antiangiogenic effect of the compounds were observed after 24 h.

### **Giemsa and ethidium bromide/acridine orange staining**

EAT cell lines were obtained from the JSS College of Pharmacy, Mysuru. The cells were centrifuged at 3000 rpm for 5 min and the packed cells were diluted 1:6 times with phosphate buffer saline. Two milliliters of the diluted cells were treated with the synthesized compounds **19**, **23** and **28** and incubated for 4 h at 37 °C. Untreated EAT cells served as control. At the end of 4 h, the samples were centrifuged, smears were made from the cell pellet obtained and fixed with methanol/acetic acid (3:1), and the morphological features of the cells were observed using different stains. Batches of both test and control smears were stained with Giemsa's stain and acridine orange/ethidium bromide stain that highlights the apoptotic morphology of the cells when observed under bright field microscope and fluorescent microscope, respectively.

### **DPPH radical scavenging activity**

Freshly prepared DPPH solution (1 mL, 0.1 mM in 95% methanol) was mixed with different aliquots of test samples (20, 40, 60, 80 and 100 µg/mL) in methanol. Ascorbic acid (AA) was used as positive control. The mixture was shaken vigorously and allowed to stand for 20 min at room temperature. The absorbance was read against a blank at 517 nm in an ELICO SL 159 UV visible spectrophotometer. The free radical scavenging potential was calculated as a percentage (*I* %) of DPPH discoloration using the Eq. (1);

$$I\% \text{ of scavenging} = (A_0 - A_1/A_0) \times 100; \quad (1)$$

where  $A_0$  is the absorbance of the control reaction mixture excluding the test compounds, and  $A_1$  is the absorbance of the test compounds.

### **Quantitative structure–activity relationship analysis**

Quantitative structure–activity relationship (QSAR) analysis was carried out to determine the variables (molecular parameters of the small molecules) that demonstrate a correlation with the potency of antioxidant activity displayed. The physicochemical properties of the small molecules synthesized in this study were computed from ChemMine tools employing OpenBabel and Joelib descriptors and ChemBioDraw 14.0. Pearson correlation coefficients were computed individually on each parameter against the obtained % radical scavenging activity and the equations were derived by linear regression with GraphPad Prism, version 4.0. The

Pearson correlation coefficients were assessed by assuming a two-tailed distribution and 95% confidence interval.

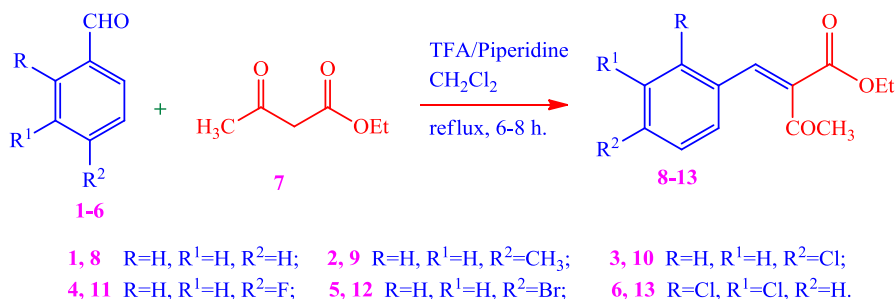
## Results and discussion

### Synthesis and characterization of compounds 8–13 and 18–29

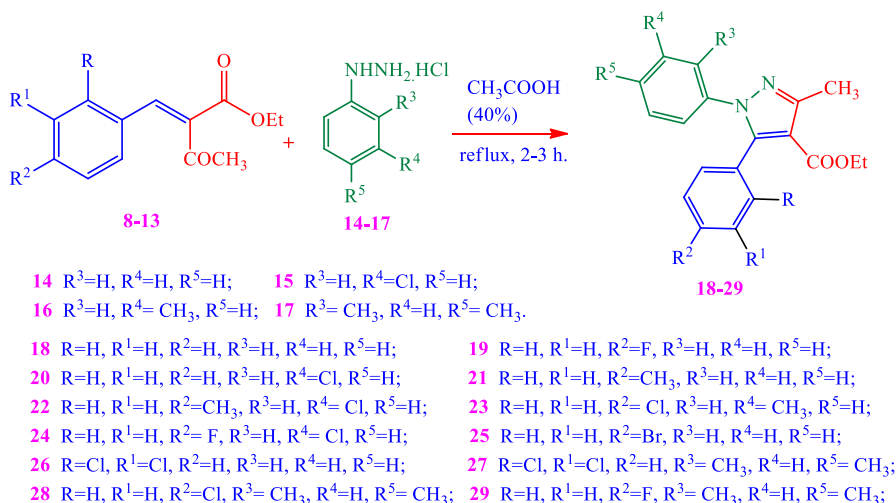
Synthesis of the target polysubstituted pyrazoles (**18–29**) was accomplished in a two-step synthetic sequence. Initially, ethyl 2-(arylidene)-3-oxobutanoates (**8–13**) were synthesized by the reaction of aromatic aldehydes (**1–6**) with ethyl acetoacetate **7** and 3–4 drops of piperidine and trifluoroacetic acid in dichloromethane under reflux conditions as is outlined in Scheme 1. The structures of **8–13** were confirmed by spectral and crystallographic studies. Earlier, we reported the crystal structures of **9** [22], **10** [23] and **11** [24] which confirms the *Z* conformation around the olefinic bond. The characterization data of compounds ethyl 2-benzylidene-3-oxobutanoate **8** [21], ethyl 2-(4-bromobenzylidene)-3-oxobutanoate **12** [25], and ethyl 2-(2,3-dichlorobenzylidene)-3-oxobutanoate **13** [26] were in agreement with the literature.

Then, the reaction of ethyl 2-(arylidene)-3-oxobutanoates (**8–13**) with phenylhydrazine hydrochlorides (**14–17**) in acetic acid under reflux conditions produced target substituted pyrazoles (**18–29**) in good yields (Scheme 2). The structures were confirmed by spectral and crystallographic studies. For instance, compound **19** shows signals at  $\delta$  1.16 ( $J = 7.0$  Hz), 2.57, 4.16 ( $J = 7.2$  Hz), 7.14–7.18 and 7.25–7.29 ppm for ester  $\text{CH}_3$ ,  $\text{CH}_3$ ,  $\text{OCH}_2$  and aromatic protons, respectively. The signals correspond to the newly formed pyrazole ring carbons viz. C-4 at  $\delta$  114.9, C-5 at  $\delta$  139.1 and C-3 at  $\delta$  151.7 ppm. Signals due to two  $\text{CH}_3$ ,  $\text{OCH}_2$  and ester  $\text{C}=\text{O}$  carbons appeared at  $\delta$  14.0, 14.2, 59.8 and 163.6 ppm, respectively. It showed a base peak at  $m/z$  325.10 corresponding to the expected molecular mass. Further, the structures of **21** [25], **19** and **25** were confirmed by crystallographic studies.

Compound **19** (CCDC: 1530834) crystallized as pale-yellow crystals suitable for single crystal X-ray diffraction (crystal size  $0.27 \times 0.25 \times 0.22$  mm) with the crystallographic parameters:  $a = 8.6121(5)$  Å,  $b = 9.8732(6)$  Å,  $c = 10.3398(6)$  Å,  $\alpha = 75.274(4)^\circ$ ,  $\beta = 73.343(4)^\circ$ ,  $\gamma = 76.295(4)^\circ$ ,  $V = 801.75(8)$  Å<sup>3</sup>,  $Z = 2$ . The



**Scheme 1** Synthesis of ethyl 2-(arylidene)-3-oxobutanoates (**8–13**)



**Scheme 2** Synthesis of functionalized pyrazoles (**18–29**)

crystal structure is triclinic with a space group of  $P - 1$  which contains pyrazole ring as a central core. Compound **25** (CCDC: 1530833) crystallized as pale-yellow crystals suitable for single crystal X-ray diffraction (crystal size  $0.29 \times 0.26 \times 0.22$  mm) with the crystallographic parameters:  $a = 10.597(2)$  Å,  $b = 19.861(4)$  Å,  $c = 8.907(2)$  Å,  $\alpha = 90.00^\circ$ ,  $\beta = 109.263(15)^\circ$ ,  $\gamma = 90.00^\circ$ ,  $V = 801.75(8)^\circ\text{Å}^3$ ,  $Z = 2$ . The crystal structure is monoclinic with a space group of  $P 21/c$  which contains pyrazole ring as the central core. The Oak Ridge Thermal-Ellipsoid Plot Program (ORTEP) diagram of molecules **19** and **25** with thermal ellipsoids drawn at 50% probability are shown in Figs. 1 and 2, respectively.

### Analytical data of compounds 18–29

**Ethyl 3-methyl-1,5-diphenyl-1H-pyrazole-4-carboxylate (18)** The characterization data was in agreement with the literature [27].

**Ethyl 5-(4-fluorophenyl)-3-methyl-1-phenyl-1H-pyrazole-4-carboxylate (19)** Yield 65%; m.p. 110–113 °C. <sup>1</sup>H NMR (CDCl<sub>3</sub>,  $\delta$  ppm): 1.16 (t, 3H,  $J = 7.0$  Hz, CH<sub>3</sub>), 2.57 (s, 3H, CH<sub>3</sub>), 4.16 (q, 2H,  $J = 7.2$  Hz, OCH<sub>2</sub>), 7.14–7.18 (m, 4H, Ar–H), 7.25–7.29 (m, 5H, Ar–H); <sup>13</sup>C NMR (CDCl<sub>3</sub>;  $\delta$  ppm): 14.0 (1C, CH<sub>3</sub>), 14.2 (1C, CH<sub>3</sub>), 59.8 (1C, OCH<sub>2</sub>), 114.9 (1C, C-4), 125.3 (2C), 126.7 (1C), 127.4 (2C), 128.5 (2C), 128.6 (2C), 130.2 (1C), 138.7 (1C), 132.4 (1C), 139.1 (1C, C-5), 151.7 (1C, C-3), 163.6 (1C, C=O). MS ( $m/z$ ): 325.10 (MH<sup>+</sup>, 100); anal. calcd. for C<sub>19</sub>H<sub>17</sub>FN<sub>2</sub>O<sub>2</sub> (%): C, 70.36; H, 5.28; N, 8.64; found: C, 70.31; H, 5.25; N, 8.61.

**Ethyl 1-(3-chlorophenyl)-3-methyl-5-phenyl-1H-pyrazole-4-carboxylate (20)** Yield 85%; m.p. 95–96 °C. <sup>1</sup>H NMR (CDCl<sub>3</sub>,  $\delta$  ppm): 1.15 (t, 3H,  $J = 7.0$  Hz, CH<sub>3</sub>), 2.57 (s, 3H, CH<sub>3</sub>), 4.16 (q, 2H,  $J = 7.2$  Hz, OCH<sub>2</sub>), 6.97–7.02 (m, 2H, Ar–H), 7.13–7.16 (m, 2H, Ar–H), 7.20–7.27 (m, 5H, Ar–H); <sup>13</sup>C NMR (CDCl<sub>3</sub>;  $\delta$  ppm): 14.1 (1C,

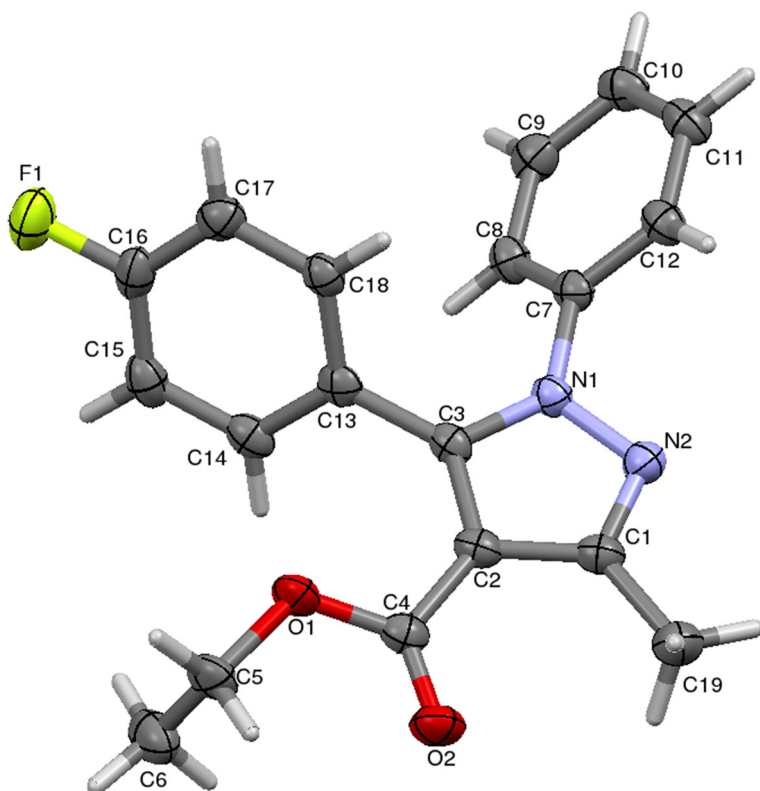


**Fig. 1** ORTEP diagram of ethyl 5-(4-fluorophenyl)-3-methyl-1-phenyl-1*H*-pyrazole-4-carboxylate **19** with thermal ellipsoids drawn at 50% probability

CH<sub>3</sub>), 14.2 (1C, CH<sub>3</sub>), 59.9 (1C, OCH<sub>2</sub>), 113.8 (1C, C-4), 116.7 (1C), 118.5 (1C), 126.4 (1C), 127.3 (2C), 128.2 (2C), 128.6 (1C), 130.9 (1C), 133.6 (1C), 134.3 (1C), 139.5 (1C, C-5), 142.4 (1C), 151.6 (1C, C-3), 163.8 (1C, C=O). MS (*m/z*): 343.01 (MH<sup>+</sup>, <sup>37</sup>Cl, 33), 341.01 (MH<sup>+</sup>, <sup>35</sup>Cl, 100); anal. calcd. for C<sub>19</sub>H<sub>17</sub>ClN<sub>2</sub>O<sub>2</sub> (%): C, 66.96; H, 5.03; N, 8.22; found: C, 66.91; H, 5.01; N, 8.20.

**Ethyl 3-methyl-1-phenyl-5-(*p*-tolyl)-1*H*-pyrazole-4-carboxylate (**21**)** [28] Yield 75%; m.p. 98 °C. <sup>1</sup>H NMR (CDCl<sub>3</sub>, δ ppm): 1.15 (t, 3H, *J* = 7.0 Hz, CH<sub>3</sub>), 2.33 (s, 3H, CH<sub>3</sub>), 2.56 (s, 3H, CH<sub>3</sub>), 4.15 (q, 2H, *J* = 7.2 Hz, OCH<sub>2</sub>), 7.08–7.13 (m, 4H, Ar-H), 7.15–7.18 (m, 2H, Ar-H), 7.21–7.26 (m, 3H, Ar-H); <sup>13</sup>CNMR (CDCl<sub>3</sub>, δ ppm): 14.0 (1C, CH<sub>3</sub>), 14.2 (1C, CH<sub>3</sub>), 21.3 (1C, Ar-CH<sub>3</sub>), 59.7 (1C, OCH<sub>2</sub>), 111.8 (1C, C-4), 125.3 (2C), 126.7 (1C), 127.4 (2C), 128.5 (2C), 128.6 (2C), 130.2 (1C), 138.7 (1C), 139.3 (1C), 146.5 (1C, C-5), 151.6 (1C, C-3), 163.8 (1C, C=O). MS (*m/z*): 321.13 (MH<sup>+</sup>, 100); anal. calcd. for C<sub>20</sub>H<sub>20</sub>N<sub>2</sub>O<sub>2</sub> (%): C, 74.98; H, 6.29; N, 8.74; found: C, 74.92; H, 6.27; N, 8.71.

**Ethyl 1-(3-chlorophenyl)-3-methyl-5-(*p*-tolyl)-1*H*-pyrazole-4-carboxylate (**22**)** Yield 73%; m.p. 135–138 °C. <sup>1</sup>H NMR (CDCl<sub>3</sub>, δ ppm): 1.16 (t, 3H, *J* = 7.0 Hz, CH<sub>3</sub>),

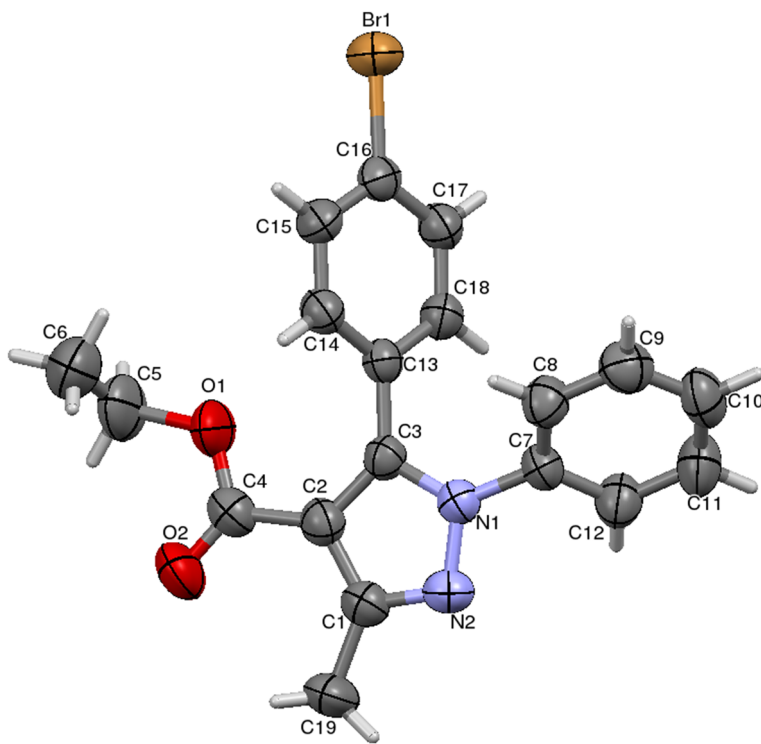


**Fig. 2** ORTEP diagram of ethyl 5-(4-bromophenyl)-3-methyl-1-phenyl-1*H*-pyrazole-4-carboxylate **25** with thermal ellipsoids drawn at 50% probability

2.33 (s, 3H, CH<sub>3</sub>), 2.57 (s, 3H, CH<sub>3</sub>), 4.15 (q, 2H,  $J = 7.2$  Hz, OCH<sub>2</sub>), 7.08–7.10 (m, 2H, Ar–H), 7.11–7.16 (m, 3H, Ar–H), 7.19–7.27 (m, 3H, Ar–H); <sup>13</sup>C NMR (CDCl<sub>3</sub>,  $\delta$  ppm): 14.1 (1C, CH<sub>3</sub>), 14.2 (1C, CH<sub>3</sub>), 21.3 (1C, Ar–CH<sub>3</sub>), 59.8 (1C, CH<sub>2</sub>), 111.3 (1C, C-4), 116.4 (1C), 118.6 (1C), 125.3 (2C), 126.1 (1C), 128.4 (2C), 130.6 (1C), 131.7 (1C), 132.2 (1C), 133.3 (1C), 140.5 (1C), 146.1 (1C, C-5), 151.4 (1C, C-3), 164.0 (1C, C=O). MS ( $m/z$ ): 357.10 (MH<sup>+</sup>, <sup>37</sup>Cl, 34), 355.08 (MH<sup>+</sup>, <sup>35</sup>Cl, 100); anal. calcd. for C<sub>20</sub>H<sub>19</sub>ClN<sub>2</sub>O<sub>2</sub> (%): C, 67.70; H, 5.40; N, 7.89; found: C, 67.68; H, 5.39; N, 7.86.

**Ethyl 5-(4-chlorophenyl)-3-methyl-1-(*m*-tolyl)-1*H*-pyrazole-4-carboxylate (**23**)** Yield 68%; m.p. 145–149 °C. <sup>1</sup>H NMR (CDCl<sub>3</sub>,  $\delta$  ppm): 1.15 (t, 3H,  $J = 7.0$  Hz, CH<sub>3</sub>), 2.24 (s, 3H, CH<sub>3</sub>), 2.56 (s, 3H, CH<sub>3</sub>), 4.16 (q, 2H,  $J = 7.2$  Hz, OCH<sub>2</sub>), 7.13–7.16 (m, 3H, Ar–H), 7.17–7.19 (m, 2H, Ar–H), 7.21–7.29 (m, 3H, Ar–H); <sup>13</sup>C NMR (CDCl<sub>3</sub>,  $\delta$  ppm): 14.0 (1C, CH<sub>3</sub>), 14.6 (1C, CH<sub>3</sub>), 21.3 (1C), 59.8 (1C, OCH<sub>2</sub>), 113.1 (1C, C-4), 116.7 (1C), 121.6 (1C), 126.2 (1C), 127.7 (2C), 128.8 (1C), 129.7 (2C), 131.0 (1C), 134.1 (1C), 138.4 (1C), 139.1 (1C), 146.5 (1C, C-5), 151.6 (1C, C-3), 163.5 (1C, C=O). MS ( $m/z$ ): 357.06 (MH<sup>+</sup>, <sup>37</sup>Cl, 33), 355.06 (MH<sup>+</sup>, <sup>35</sup>Cl, 100); anal. calcd. for C<sub>20</sub>H<sub>19</sub>ClN<sub>2</sub>O<sub>2</sub> (%): C, 67.70; H, 5.40; N, 7.89; found: C, 67.64; H, 5.39; N, 7.86.

**Ethyl 1-(3-chlorophenyl)-5-(4-fluorophenyl)-3-methyl-1H-pyrazole-4-carboxylate (24)** Yield 85%; m.p. 56–58 °C.  $^1\text{H}$  NMR ( $\text{CDCl}_3$ ,  $\delta$  ppm): 1.15 (t, 3H,  $J = 7.0$  Hz,  $\text{CH}_3$ ), 2.56 (s, 3H,  $\text{CH}_3$ ), 4.16 (q, 2H,  $J = 7.2$  Hz,  $\text{OCH}_2$ ), 6.97–6.99 (m, 2H, Ar–H), 7.12–7.19 (m, 3H, Ar–H), 7.21–7.26 (m, 3H, Ar–H);  $^{13}\text{C}$  NMR ( $\text{CDCl}_3$ ,  $\delta$  ppm): 14.1 (1C,  $\text{CH}_3$ ), 14.4 (1C,  $\text{CH}_3$ ), 60.1 (1C,  $\text{OCH}_2$ ), 113.8 (1C, C-4), 116.7 (1C), 117.3 (2C), 118.8 (1C), 126.4 (1C), 128.3 (1C), 130.5 (2C), 131.1 (1C), 134.2 (1C), 140.1 (1C, C-5), 141.6 (1C), 151.6 (1C, C-3), 162.1 (1C), 163.4 (1C, C=O). MS ( $m/z$ ): 361.06 ( $\text{MH}^+$ ,  $^{37}\text{Cl}$ , 34), 359.04 ( $\text{MH}^+$ ,  $^{35}\text{Cl}$ , 100); anal. calcd. for  $\text{C}_{19}\text{H}_{16}\text{ClFN}_2\text{O}_2$  (%): C, 63.60; H, 4.49; N, 7.81; found: C, 63.57; H, 4.48; N, 7.78.

**Ethyl 5-(4-bromophenyl)-3-methyl-1-phenyl-1H-pyrazole-4-carboxylate (25)** Yield 80%; m.p. 87–88 °C.  $^1\text{H}$  NMR ( $\text{CDCl}_3$ ,  $\delta$  ppm): 1.16 (t, 3H,  $J = 7.0$  Hz,  $\text{CH}_3$ ), 2.57 (s, 3H,  $\text{CH}_3$ ), 4.15 (q, 2H,  $J = 7.2$  Hz,  $\text{OCH}_2$ ), 7.11 (dd, 2H,  $J = 6.8$ ,  $J = 1.6$  Hz, Ar–H), 7.14 (m, 2H,  $J = 6.2$ ,  $J = 1.2$  Hz, Ar–H), 7.24–7.27 (m, 3H, Ar–H), 7.42–7.44 (m, 2H, Ar–H);  $^{13}\text{C}$  NMR ( $\text{CDCl}_3$ ,  $\delta$  ppm): 14.1 (1C,  $\text{CH}_3$ ), 14.5 (1C,  $\text{CH}_3$ ), 60.0 (1C,  $\text{OCH}_2$ ), 112.9 (1C, C-4), 123.7 (1C), 124.5 (2C), 125.8 (1C), 128.5 (2C), 129.7 (2C), 131.8 (2C), 132.4 (1C), 138.3 (1C), 141.6 (1C, C-5), 151.2 (1C, C-3), 163.3 (1C, C=O). MS ( $m/z$ ): 387.02 ( $\text{MH}^+$ ,  $^{81}\text{Br}$ , 98), 384.01 ( $\text{MH}^+$ ,  $^{79}\text{Br}$ , 100); anal. calcd. for  $\text{C}_{19}\text{H}_{17}\text{BrN}_2\text{O}_2$  (%): C, 59.23; H, 4.45; N, 7.27; found: C, 59.20; H, 4.44; N, 7.25.

**Ethyl 5-(2,3-dichlorophenyl)-3-methyl-1-phenyl-1H-pyrazole-4-carboxylate (26)** Yield 65%; m.p. 51–53 °C.  $^1\text{H}$  NMR ( $\text{CDCl}_3$ ,  $\delta$  ppm): 1.14 (t, 3H,  $J = 7.0$  Hz,  $\text{CH}_3$ ), 2.54 (s, 3H,  $\text{CH}_3$ ), 4.17 (q, 2H,  $J = 7.2$  Hz,  $\text{OCH}_2$ ), 6.97–6.99 (m, 2H, Ar–H), 7.00–7.16 (m, 3H, Ar–H), 7.20–7.24 (m, 4H, Ar–H);  $^{13}\text{C}$  NMR ( $\text{CDCl}_3$ ,  $\delta$  ppm): 14.0 (1C,  $\text{CH}_3$ ), 14.6 (1C,  $\text{CH}_3$ ), 60.2 (1C,  $\text{OCH}_2$ ), 113.5 (1C, C-4), 124.4 (2C), 126.3 (1C), 127.1 (1C), 127.6 (1C), 129.2 (2C), 130.1 (1C), 131.3 (1C), 131.8 (1C), 132.9 (1C), 139.1 (1C), 141.9 (1C, C-5), 151.7 (1C, C-3), 163.0 (1C, C=O). MS ( $m/z$ ): 378.01 ( $\text{M} + 4$ , 11), 376.02 ( $\text{M} + 2$ , 63), 374.05 ( $\text{M}^+$ , 100); anal. calcd. for  $\text{C}_{19}\text{H}_{16}\text{Cl}_2\text{N}_2\text{O}_2$  (%): C, 60.81; H, 4.30; N, 7.47; found: C, 60.76; H, 4.29; N, 7.45.

**Ethyl 5-(2,3-dichlorophenyl)-1-(2,4-dimethylphenyl)-3-methyl-1H-pyrazole-4-carboxylate (27)** Yield 65%; m.p. 45–47 °C.  $^1\text{H}$  NMR ( $\text{CDCl}_3$ ,  $\delta$  ppm): 1.16 (t, 3H,  $J = 7.0$  Hz,  $\text{CH}_3$ ), 1.97 (s, 3H,  $\text{CH}_3$ ), 2.32 (s, 3H,  $\text{CH}_3$ ), 2.54 (s, 3H,  $\text{CH}_3$ ), 4.18 (q, 2H,  $J = 7.2$  Hz,  $\text{OCH}_2$ ), 7.15–7.20 (m, 3H, Ar–H), 7.24–7.29 (m, 3H, Ar–H);  $^{13}\text{C}$  NMR ( $\text{CDCl}_3$ ,  $\delta$  ppm): 14.0 (1C,  $\text{CH}_3$ ), 14.3 (1C,  $\text{CH}_3$ ), 40.7 (2C,  $\text{NCH}_3$ ), 60.2 (1C,  $\text{OCH}_2$ ), 113.4 (1C, C-4), 120.1 (1C), 123.8 (1C), 125.8 (1C), 126.1 (1C), 127.3 (1C), 130.1 (1C), 131.1 (1C), 132.0 (1C), 133.1 (1C), 135.0 (2C), 139.6 (1C), 141.5 (1C, C-5), 151.6 (1C, C-3), 163.3 (1C, C=O). MS ( $m/z$ ): 406.09 ( $\text{M} + 4$ , 13), 404.08 ( $\text{M} + 2$ , 64), 402.10 ( $\text{M}^+$ , 100); anal. calcd. for  $\text{C}_{21}\text{H}_{20}\text{Cl}_2\text{N}_2\text{O}_2$  (%): C, 62.54; H, 5.00; N, 6.95; found: C, 62.51; H, 4.98; N, 6.93.

**Ethyl 5-(4-chlorophenyl)-1-(2,4-dimethylphenyl)-3-methyl-1H-pyrazole-4-carboxylate (28)** Semi-solid, yield 68%.  $^1\text{H}$  NMR ( $\text{CDCl}_3$ ,  $\delta$  ppm): 1.19 (t, 3H,  $J = 7.0$  Hz,  $\text{CH}_3$ ), 1.94 (s, 3H,  $\text{CH}_3$ ), 2.30 (s, 3H,  $\text{CH}_3$ ), 2.53 (s, 3H,  $\text{CH}_3$ ), 4.19 (q, 2H,  $J = 7.2$  Hz,  $\text{OCH}_2$ ), 7.28–7.39 (m, 3H, Ar–H), 7.56–7.59 (m, 4H, Ar–H);  $^{13}\text{C}$  NMR ( $\text{CDCl}_3$ ,  $\delta$  ppm): 14.1 (1C,  $\text{CH}_3$ ), 14.3 (1C,  $\text{CH}_3$ ), 15.5 (1C,  $\text{CH}_3$ ), 20.7 (1C,

CH<sub>3</sub>), 60.3 (1C, OCH<sub>2</sub>), 112.5 (1C, C-4), 118.6 (1C), 123.2 (1C), 125.6 (1C), 128.8 (2C), 129.3 (2C), 130.0 (1C), 133.9 (1C), 134.7 (1C), 136.3 (1C), 140.1 (1C), 141.8 (1C, C-5), 151.2 (1C, C-3), 163.1 (1C, C=O). MS (*m/z*): 370.09 (M+, <sup>37</sup>Cl, 34), 368.10 (M+, <sup>35</sup>Cl, 100); anal. calcd. for C<sub>21</sub>H<sub>21</sub>ClN<sub>2</sub>O<sub>2</sub> (%): C, 68.38; H, 5.74; N, 7.59; found: C, 68.31; H, 5.73; N, 7.57.

**Ethyl 1-(2,4-dimethylphenyl)-5-(4-fluorophenyl)-3-methyl-1H-pyrazole-4-carboxylate (29)** Semi-solid, yield 70%. <sup>1</sup>H NMR (CDCl<sub>3</sub>, δ ppm): 1.21 (t, 3H, *J* = 7.0 Hz, CH<sub>3</sub>), 1.95 (s, 3H, CH<sub>3</sub>), 2.31 (s, 3H, CH<sub>3</sub>), 2.54 (s, 3H, CH<sub>3</sub>), 4.21 (q, 2H, *J* = 7.2 Hz, OCH<sub>2</sub>), 7.29–7.37 (m, 3H, Ar–H), 7.57–7.60 (m, 4H, Ar–H); <sup>13</sup>C NMR (CDCl<sub>3</sub>, δ ppm): 14.2 (1C, CH<sub>3</sub>), 14.3 (1C, CH<sub>3</sub>), 15.7 (1C, CH<sub>3</sub>), 20.9 (1C, CH<sub>3</sub>), 60.3 (1C, OCH<sub>2</sub>), 112.4 (1C, C-4), 117.8 (2C), 118.5 (1C), 122.10 (1C), 125.7 (1C), 128.2 (1C), 129.8 (2C), 134.7 (1C), 135.3 (1C), 140.1 (1C), 141.6 (1C, C-5), 151.3 (1C, C-3), 159.4 (1C), 163.2 (1C, C=O). MS (*m/z*): 352.11 (M+, 100); anal. calcd. for C<sub>21</sub>H<sub>21</sub>FN<sub>2</sub>O<sub>2</sub> (%): C, 71.57; H, 6.01; N, 7.95; found: C, 71.54; H, 5.99; N, 7.93.

### Anti-angiogenic activity of compounds 18–29

In order to evaluate the anti-angiogenic activity of the pyrazole derivatives **18–29**, we first assessed their *in vitro* cytotoxic effect on MCF-7 breast cancer cell lines following 48 h of exposure using trypan blue and (3-(4,5-dimethylthiazol-2-yl)-2,5-diphenyltetrazolium bromide (MTT) [29]. This *in vitro* screening is performed to identify the compounds amongst the series that exhibit cytotoxic effects. Tamoxifen (TMX) was used as a standard, and DMSO as negative control; the results of the screening are summarized in Table 2. In the trypan blue assay, compounds **19**, **23** and **28** showed excellent cell growth inhibition with IC<sub>50</sub> values of 7.9, 10.6 and 8.2 μM, respectively, in comparison with the standard TMX's 11.4 μM. The effect of compounds on cell proliferation tested using MTT assay reveals that, compounds **19**, **23** and **28** have maximum cytotoxic effect with IC<sub>50</sub> values of 7.6, 10.4 and 8.5 μM, respectively. These results were in agreement with those reported with trypan blue (Table 2).

Obviously, from the results, compound **19** (7.9 μM) with fluoro substitution at the para position of the phenyl ring exhibited the highest activity against MCF-7 cells in trypan blue with MTT assay IC<sub>50</sub> values of 7.9 and 7.6 μM when compared with the standard. The results reveal that compounds **26** and **27** have no cytotoxic effect and compounds **18**, **20**, **24** and **29** possess moderate cytotoxic effects on MCF-7 cells. Compounds **19**, **23** and **28** were considered as lead compounds for further investigation. The cytotoxic effects of synthesized pyrazole derivatives **18–29** on MCF-7 cell lines were well within the range exhibited by similar and structurally related pyrazoles [29].

To study the morphological features of the cells, we subjected the cells to Giemsa and ethidium bromide/acridine orange staining [30]. In this, experimental batches of both test and control smears were stained with Giemsa's stain and acridine orange/ethidium bromide stain that highlights the apoptotic morphology of the cells when observed under florescent microscope and as photographed employing a Nikon

**Table 2** IC<sub>50</sub> values of designed series of compounds **18–29** on trypan blue and MTT assay at 48 h in MCF-7 cells

Compounds	Trypan blue assay IC <sub>50</sub> value (μM)	MTT assay IC <sub>50</sub> value (μM)
Negative control	–	–
18	19 ± 0.27	21 ± 0.18
<b>19</b>	<b>7.9 ± 0.07</b>	<b>7.6 ± 0.08</b>
20	17 ± 0.17	16 ± 0.22
21	44 ± 0.12	49 ± 0.16
22	71 ± 0.19	65 ± 0.13
<b>23</b>	<b>10.6 ± 0.07</b>	<b>10.4 ± 0.08</b>
24	14 ± 0.11	13 ± 0.12
25	84 ± 0.25	87 ± 0.19
26	> 100	> 100
27	> 100	> 100
<b>28</b>	<b>8.2 ± 0.13</b>	<b>8.5 ± 0.16</b>
29	19 ± 0.15	21 ± 0.20
Positive control	<b>11.4 ± 0.07</b>	<b>11.4 ± 0.09</b>

Based on the IC<sub>50</sub> values, compounds **19**, **23** and **28** were chosen as lead compounds as indicated by IC<sub>50</sub> values in bold entries

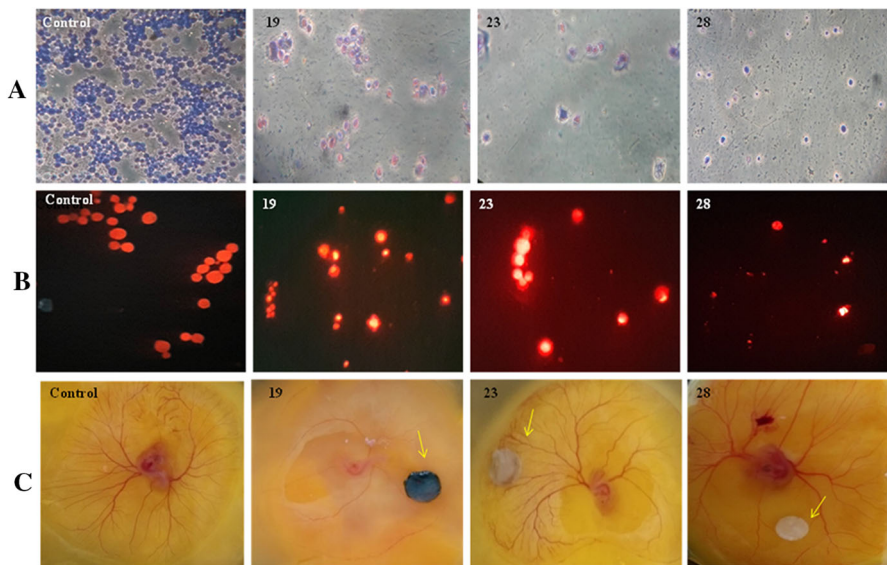


**Fig. 3** Cytotoxic and antiangiogenic effect of compounds **19**, **23** and **28**. (A) Giemsa staining of normal cells and cells treated with compounds **19**, **23** and **28** highlighting widespread cell death. (B) Ethidium bromide/acridine orange staining of normal cells and cells treated with compounds **19**, **23** and **28** highlighting cell death. (C) CAM photos illustrates the formation of blood vessels in normal cells with regression of angiogenesis in cells treated with compounds **19**, **23** and **28**

D3200 camera (Fig. 3a, b). The apoptotic morphology clearly indicated the potential cytotoxic effect of compounds **19**, **23** and **28**.

The anti-angiogenic activity of the designed series of pyrazoles **18–29** was evaluated in the shell less CAM assay [30], which is the most widely used assay to study angiogenesis in vivo. In this model, compounds **18–29** induced moderate to good aviculture zone formation in the developing embryos. Amongst the tested compounds, compound **19**, **23** and **28** clearly show regression of newly formed micro-vessels which were found around the area of disc implantation compared to the other compounds in the series (Fig. 3c). This regression of micro-vessel density in the CAM model is highly evident of inhibition of angiogenesis and it correlates with our in vitro results more accurately.

### DPPH radical scavenging activity of compounds 18–29

As an additional investigation, we also performed the DPPH radical scavenging assay of the synthesized compounds **18–29** according to Blois method [31, 32]. The results were expressed as  $I\% \pm$  standard deviations (SD;  $n = 3$ ). The results of the findings (Table 3) clearly showed that the newly synthesized compounds exhibited good activities. Preliminary investigation results reveal that compounds **20**, **24** and **26** with chlorophenyl substitutions of the pyrazole showed stronger DPPH scavenging activity in comparison with the standard ascorbic acid. Compounds **19**, **23** and **28** showed scavenging abilities similar to that displayed by the standard. However, the rest of the compounds showed lesser activities. From these results, it

**Table 3** DPPH radical scavenging activity of the synthesized pyrazoles **18–29**

Compounds	% Radical scavenging activity <sup>a</sup>				
	20 (µg/mL)	40 (µg/mL)	60 (µg/mL)	80 (µg/mL)	100 (µg/mL)
<b>18</b>	15.21 ± 0.65	16.12 ± 0.87	21.12 ± 0.41	24.22 ± 0.32	26.08 ± 0.41
<b>19</b>	18.45 ± 0.11	20.16 ± 0.98	23.67 ± 0.11	25.65 ± 0.76	28.94 ± 0.20
<b>20</b>	23.54 ± 0.21	24.56 ± 0.76	29.21 ± 0.41	31.54 ± 0.32	34.65 ± 0.41
<b>21</b>	14.12 ± 0.87	13.99 ± 0.43	19.76 ± 0.32	22.54 ± 0.12	23.95 ± 0.31
<b>22</b>	15.61 ± 0.21	17.34 ± 0.76	23.45 ± 0.51	24.98 ± 0.54	27.95 ± 0.56
<b>23</b>	16.98 ± 0.28	18.97 ± 0.32	23.76 ± 0.58	25.75 ± 0.42	28.07 ± 0.71
<b>24</b>	19.03 ± 0.87	20.98 ± 0.10	24.84 ± 0.32	27.76 ± 0.11	29.87 ± 0.32
<b>25</b>	17.22 ± 0.32	17.96 ± 0.89	20.54 ± 0.76	22.05 ± 0.32	25.76 ± 0.26
<b>26</b>	23.54 ± 0.21	24.56 ± 0.76	29.21 ± 0.41	31.54 ± 0.32	34.65 ± 0.41
<b>27</b>	14.01 ± 0.32	16.21 ± 0.97	21.03 ± 1.01	23.11 ± 0.50	26.05 ± 0.63
<b>28</b>	17.35 ± 0.26	18.90 ± 0.55	22.34 ± 0.35	25.24 ± 0.50	28.75 ± 0.65
<b>29</b>	13.98 ± 0.40	15.30 ± 0.40	20.16 ± 0.86	23.08 ± 0.75	25.35 ± 0.82
AA <sup>b</sup>	15.08 ± 0.89	16.87 ± 0.89	21.98 ± 0.31	24.25 ± 0.22	28.65 ± 0.98

<sup>a</sup>Values are mean ± SD of three replicates ( $n = 3$ )

<sup>b</sup>Ascorbic acid = positive control

is anticipated that the presence of a monochloro-substituted phenyl ring at the 1 position of the pyrazole ring influences the increasing DPPH radical scavenging abilities of the designed series of pyrazoles.

### Quantitative structure–activity relationship analysis

To understand the potential molecular features that were contributing towards the potency of the observed antioxidant activity by some of the compounds, a systematic QSAR analysis was carried out. A pairwise analysis on a total of 38 molecular parameters was assessed for possible correlation with the potency of observed antioxidant activity for the 12 compounds reported (18–29; Fig. 4). The molecular parameters included, but are not limited to, variables such as the molecular weight, Log*P*, presence/absence of various halogenated substituents, hydrogen bonding donors/acceptors, presence and number of single and double

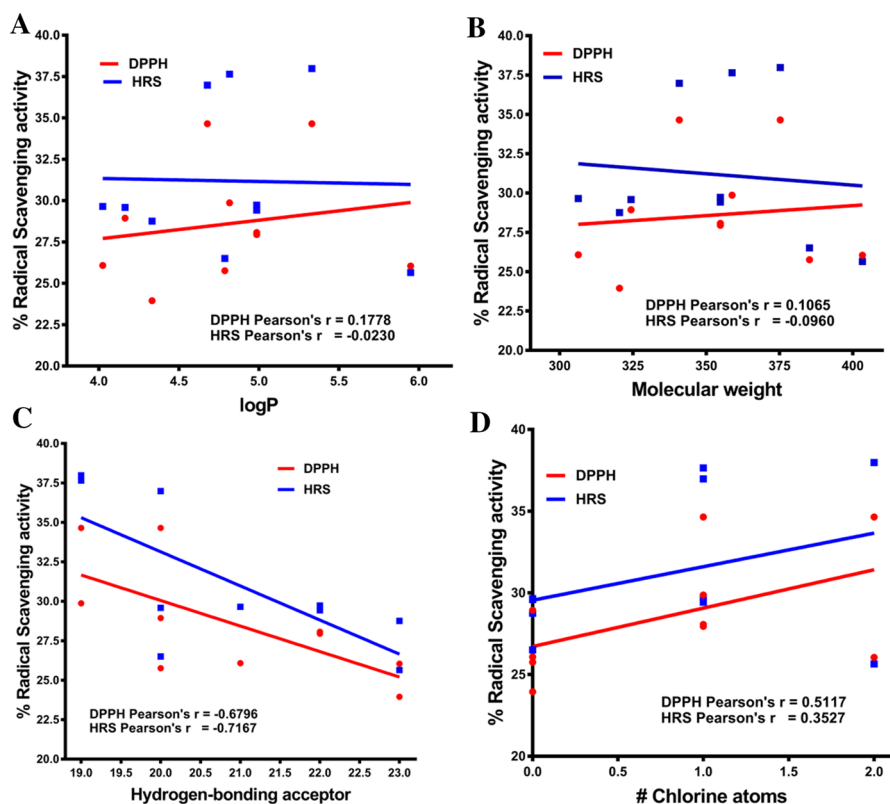


**Fig. 4** Pairwise correlation analysis for four different physicochemical parameters computed for compounds from series 18–29 against the DPPH and hydroxyl radical scavenging activity (HRS). In the plots, the y-axis represents the % radical scavenging activity and the x-axis indicates the various physicochemical parameters computed for compounds employing Joelib and OpenBabel. The plots were generated in GraphPad Prism, version 4.0, and the linear regression and correlation analysis were carried out using the functions employed by the software. “Pearson’s  $r$  indicates the correlation coefficient

bonds, molecular connectivity parameters like Zagreb group index, shape, etc. Before discussing the obtained results, it would be appropriate to point out that the 12 molecules designed and synthesized in this study share a highly conserved invariable core with minor aliphatic and halogenated substitutions. Hence, the minor variability in the microenvironment of the small molecules translating into potency of antioxidant activity presents an appropriate exercise in modeling an accurate QSAR model.

The pairwise comparison shows that, among other parameters, the potency of the antioxidant activity doesn't correlate with parameters like  $\text{Log}P$  and the molecular weight of the synthesized compounds (Fig. 4a, b). However, the hydrogen bonding acceptor 1 parameter correlated negatively with the potency of antioxidant activity having a reasonably good Pearson's correlation coefficient with a  $P$  value less than 0.04, indicating reasonable significance (Fig. 4c). This indicates that in the current series of compounds, the lesser the hydrogen bonding acceptance potential of a small molecule, the greater the possibility that it will have potent antioxidant activity. The parameter that showed positive correlation with the potency of antioxidant activity was the content of the halide chlorine (Fig. 4d). However, the statistics of the correlation was not very strong, indicating that chloride substitution's effect on potency is highly regional. For instance, compound **27**, in spite of having two chlorine substitutions, showed relatively less potent antioxidant activity.

Future studies would attempt the synthesis of further compounds in this series for the sake of statistical rigor of the analysis. Two-dimensional QSAR analysis employing both multiple linear regressions (MLR) and partial least square regression (PLR) would be attempted. As an additional measure, depending on the availability of crystal structure information for all the synthesized compounds in the series, three-dimensional QSAR strategies using comparative molecular field analysis (CoMFA) and comparative molecular similarity index analysis (CoMSIA) would also be attempted. However, it would have to be pointed out that the success of QSAR predictions, to a large extent, depend on the training set and it would be important to implement rigorous training subroutines employing either genetic algorithms or far more traditional approaches.

## Conclusions

To sum up, in the present work, we report a procedure for the direct synthesis of pyrazoles from various ethyl 2-(4-aryl)-3-oxobutanoates. The ethyl ester function in a substituted pyrazole ring is posited to be the key feature for the biological potency of the synthesized compounds. From the results of the biological evaluation, it is evident that amongst the designed series, compounds **19**, **24** and **28** exhibit promising cytotoxic and angiogenic properties; compounds, **20**, **24** and **26** possess good antioxidant properties. The demonstrated synthesis paves the way for future efforts at synthesizing derivatives of pyrazoles that could find widespread applications in medicinal chemistry and efforts aimed at alleviating the dreadful outcomes that oxidative stress imposes.

**Acknowledgements** The authors are grateful to the IOE Instrumentation Facility, Vijnana Bhavana, University of Mysore, for recording spectra and X-ray diffraction studies, and JSS College of Pharmacy, Mysuru, for providing cell lines.

### Compliance with ethical standards

**Conflict of interest** All authors declare no conflict of interest including financial, personal or other relationships with other people or organizations for this article.

## References

1. S. Eckhardt, *Curr. Med. Chem.* **3**, 419 (2002)
2. R. Katoch-Rouse, O.A. Pavlova, T. Caulder, A.F. Hoffmann, A.G. Mukhin, A.G. Horti, *J. Med. Chem.* **46**, 642 (2003)
3. O. Bruno, F. Bondavalli, A. Ranise, P. Schenone, C. Losasso, L. Cilenti, C. Matera, E. Marmo, *Farmaco* **45**, 147 (1990)
4. D.M. Lokeshwari, D.K. Achutha, B. Srinivasan, N. Shivalingegowda, L.N. Krishnappagowda, A.K. Kariyappa, *Bioorg. Med. Chem. Lett.* **27**, 3806 (2017)
5. Z. Sui, J. Guan, M.P. Ferro, K. McCoy, M.P. Wachter, W.V. Murray, M. Singer, M. Steber, D.M. Ritchie, D.C. Argentieri, *Bioorg. Med. Chem. Lett.* **10**, 601 (2000)
6. J.S. Pasin, A.P. Ferreira, A.L. Saraiva, V. Ratzlaff, R. Andrighetto, P. Machado, S. Marchesan, R.A. Zanette, H.G. Bonacorso, N. Zanatta, M.A. Maritins, J. Ferreira, C.F. Mello, *Braz. J. Med. Biol. Res.* **43**, 1193 (2010)
7. S.R. Stauffer, C.J. Coletta, R. Tedesco, G. Nishiguchi, K. Carlson, J. Sun, B.S. Katzenellenbogen, J.A. Katzenellenbogen, *J. Med. Chem.* **43**, 4934 (2000)
8. M.J. Ahsan, *Arab. J. Chem.* **10**, S2762 (2017)
9. D. Secci, A. Bolasco, P. Chimenti, S. Carradori, *Curr. Med. Chem.* **18**, 5114 (2011)
10. A.D. Prasanna, R.J. Sonali, *Int. J. Med. Chem.* **2015**, 670181 (2015)
11. L.D. Mahadevaswamy, A.K. Kariyappa, *Pharm. Chem. J.* **51**, 670 (2017)
12. C. Lamberth, *Heterocycles* **71**, 1467 (2007)
13. J. Prabhaskar, V.K. Govindappa, A.K. Kariyappa, *Turk. J. Chem.* **37**, 853 (2013)
14. K. Mohanan, A.R. Martin, L. Toupet, M. Smietana, J.-J. Vasseur, *Angew. Chem. Int. Ed.* **49**, 3196 (2010)
15. O.K. Yang, Y.S. Chun, C.-L. Park, Y. Kim, H. Shin, S. Ahn, J. Hong, S. Lee, *Org. Biomol. Chem.* **7**, 1132 (2009)
16. P. Jayaroopa, K. Ajay Kumar, *Int. J. Pharm. Pharm. Sci.* **5**(4), 431 (2013)
17. A.R. Katrizky, M. Wang, S. Zhang, M.V. Voronkov, *J. Org. Chem.* **66**, 6787 (2001)
18. D. Ribatti, A. Vacca, L. Roncali, F. Dammacco, *Haematologica* **76**, 311 (1991)
19. R. Domenico, V. Angelo, R. Luisa, D. Franco, *Curr. Pharm. Biotechnol.* **1**, 73 (2000)
20. M.E. Buyukokuroglu, I. Gulcin, M. Oktay, O.I. Kufrevioglu, *Pharmacol. Res.* **44**, 491 (2001)
21. A.I. Ismiyev, *Acta Crystallogr. Sect. E Struct. Rep Online* **E67**, o1863 (2011)
22. A.K. Kariyappa, N. Shivalingegowda, D.K. Achutha, N.K. Lokanath, *Chem. Data Collect.* **3–4**, 1 (2016)
23. A. Dileep Kumar, S. Naveen, H.K. Vivek, M. Prabhswamy, N.K. Lokanath, K. Ajay Kumar, *Chem. Data Collect.* **5–6**, 36 (2016)
24. A. Dileep Kumar, K. Kumara, N.K. Lokanath, K. Ajay Kumar, M. Prabhswamy, *Chem. Data Collect.* **5–6**, 68 (2016)
25. S. Hong, Y. Shin, M. Jung, M.W. Ha, Y. Park, Y.-J. Lee, J. Shin, K.B. Oh, S.K. Lee, H.-G. Park, *Eur. J. Med. Chem.* **96**, 218 (2015)
26. W.H. Correa, J.L. Scott, *Green Chem.* **3**, 296 (2001)
27. Chandra, N. Srikantamurthy, E.A. Jithesh Babu, K.B. Umesha, M. Mahendra, *AIP Conf. Proc.* **1591**, 1197 (2014)
28. S. Naveen, A. Dileep Kumar, K. Kumara, K. Ajay Kumar, N.K. Lokanath, I. Warad, *IUCrData* **1**, x161972 (2016)
29. S.C. Michael, L. Sandra, M.K. Konstantinos, A.H. Serkos, *Bioorg. Med. Chem.* **18**, 4338 (2010)

30. V.L. Ranganatha, F. Zameer, S. Meghashri, N.D. Rekha, V. Girish, H.D. Gurupadaswamy, S.A. Khanum, Arch. Pharm. Chem. Life Sci. **346**, 901 (2013)
31. M.S. Blois, Nature **181**, 1199 (1958)
32. N. Renuka, H.K. Vivek, G. Pavithra, K. Ajay Kumar, Russ. J. Bioorg. Chem. **43**, 197 (2017)